Near-Optimal Swapping and Purifying Strategy for All-Optical-Switching Entanglement Routing

Shao-Min Huang[§†‡], Tang-Ming Hsu[§‡], Jing-Jhih Du[‡], Jian-Jhih Kuo[*‡], and Chih-Yu Wang[†]
[†]Research Center for Information Technology Innovation, Academia Sinica, Taipei City, Taiwan
[‡]Dept. of Computer Science and Information Engineering, National Chung Cheng University, Chiayi, Taiwan

***Abstract*—Entangled pairs serve as the cornerstone for secure data transmission. All-optical-switching technology on nodes enables the entangling signals to bypass nodes and build ultra-long entangled pairs. Nevertheless, entangled pairs suffer from decoherence over distance, causing inadequate fidelity and potentially compromising transmission quality. To address the challenges, we employ entanglement purification to enhance fidelity to meet the threshold. However, the purification process consumes additional entangled pairs and may fail. Besides, the purification efficiency would be poor if the input pairs have low fidelity. Thus, it is unavoidable to divide the path into sub-paths with appropriate lengths for better purification efficiency and then merge them into a longer entangled pair by swapping. The novel optimization problem DOSP then emerges: maximizing the probability while adhering to fidelity constraints. To tackle the DOSP efficiently, we propose a $(1-\delta)$-approximation algorithm NSPS to consider the probability and fidelity jointly, where δ is a positive user-defined constant. Finally, the simulation results manifest that the NSPS can outperform the existing methods by at least 70%.**

I. Introduction

Quantum networks (QNs) promise to facilitate secure data transmission and enable various innovative applications in information and communication technology. Within a QN, quantum nodes (circles) are interconnected by quantum channels (represented by black solid lines) to transmit quantum information in the form of *qubits* [1], as depicted in Fig. 1. Each quantum node in the QN possesses a specific amount of quantum memory (blue squares) to store qubits and mitigate rapid decoherence [2]. Fibers (black lines) allows adjacent pairs to produce entangled pairs (red dots). Furthermore, by adopting all-optical-switching technology, entangling signals can bypass quantum nodes to generate longer pairs. However, exploiting the bypassing strategy may cause unacceptable fidelity when the distance within an bypassed end-to-end entangled pair is too long. To overcome this defect, entanglement purification can be exploited to consume a sacrifice pair and enhance the target pair's fidelity [3]. Nevertheless, conducting entanglement purification for a target pair will be efficient only when the original fidelity of the pair is with in a certain range. This range suggests the proper choice of the length of the entanglement pair. Thus, it is necessary to divide the routing path into a suitable number of sub-paths, generate and purify the target pair for each sub-path individually, and eventually merge them into an end-to-end entangled pair by entanglement swapping.

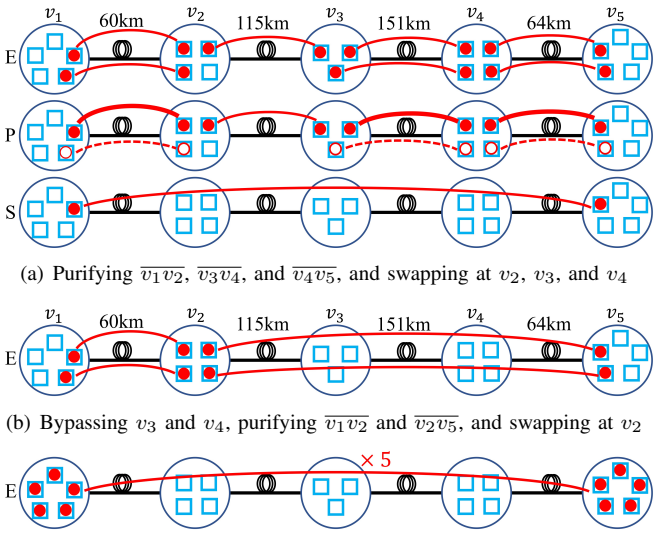

(a) Purifying $\overline{v_1v_2}$, $\overline{v_3v_4}$, and $\overline{v_4v_5}$, and swapping at v_2, v_3, and v_4

(b) Bypassing v_3 and v_4, purifying $\overline{v_1v_2}$ and $\overline{v_2v_5}$, and swapping at v_2

(c) Complete bypassing strategy

Fig. 1. Illustration of different swapping and purifying strategies.

Fig. 1(a) illustrates the process of generating an end-to-end entangled pair from v_1 to v_5. Firstly, during the entangling phase, entangled pairs are generated. Longer entangled pairs have less fidelity, and the fidelity of $(\overline{v_1v_2}, \overline{v_2v_3}, \overline{v_3v_4}, \overline{v_4v_5}) = (0.89, 0.8, 0.76, 0.88)$. Among these pairs, $\overline{v_1v_2}$, $\overline{v_3v_4}$, and $\overline{v_4v_5}$ generate extra entangled pairs to undergo purification in the subsequent phase. Secondly, in the purification phase, $\overline{v_1v_2}$, $\overline{v_3v_4}$, and $\overline{v_4v_5}$ conduct a single purification process, consuming a sacrifice pair (dotted red line) to enhance the target pair's fidelity. After that, the fidelity of $(\overline{v_1v_2}, \overline{v_3v_4}, \overline{v_4v_5})$ becomes $(0.98, 0.91, 0.98)$. It is worth noting that the purification process has a success probability contingent upon the fidelity of the input pairs, i.e., it could fail. Thirdly, in the swapping phase, quantum nodes execute entanglement swapping to combine the short pairs into an end-to-end pair. However, similar to the purification process, there is a chance of failure during swapping. Also, the swapping process may result in a reduction in fidelity. In the end, the overall fidelity of the end-to-end pair is measured to be 0.71 in the example.

Figs. 1(b) and 1(c) illustrate two alternative strategies. In Fig. 1(b), the strategy opts to bypass v_3 and v_4 to directly generate $\overline{v_2v_5}$ with a length of $115+151+64$, leading to the fidelity of 0.62. After a single purification process, $\overline{v_1v_2}$ and $\overline{v_2v_5}$ have the

§: equal contributions; *: corresponding author (lajacky@cs.ccu.edu.tw)
This work was supported by the National Science and Technology Council under Grants 111-2628-E-001-002-MY3, 111-2628-E-194-001-MY3, 112-2218-E-194-005, 113-2221-E-194-040-MY3, and the Academia Sinica under Thematic Research Grant AS-TP-110-M07-3 in Taiwan.

purified fidelity of 0.98 and 0.73 (detailed later), respectively. On the other hand, Fig. 1(c) decides to bypass all the repeaters and connect the end-to-end pairs $\overline{v_1v_5}$ directly, resulting in a fidelity of 0.72. Subsequently, a pumping strategy is employed to purify the target pair by performing four single purification processes sequentially, resulting in the fidelity of 0.87. If the end-to-end fidelity threshold is set to 0.7, all the three cases in Fig. 1 meet the fidelity threshold. Fig. 1(c) exhibits the highest fidelity among the three. However, each case has a different probability.[1] Specifically, the success probabilities for Figs. 1(a)$-$1(c) are 0.22, 0.31, and 0.06, respectively. Considering fidelity and probability jointly, Fig. 1(b) emerges as the best choice among them. Although Fig. 1(c) boasts the highest fidelity, it suffers from the lowest probability. By contrast, Fig. 1(b) strikes a balance between fidelity and probability, making it the optimal choice among the options.

In this paper, we first attempt to explore fidelity decrease toward distance while taking purification into account to meet the fidelity threshold. This exploration introduces several challenges: 1) *Purification gain vs current fidelity*. The purification process can enhance fidelity, but the extent of improvement corresponds to the fidelity of the input pairs. The maximum gain occurs at around 0.74 fidelity and diminishes as fidelity approaches 0.5 or 1. It means that purifying a non-bypassing short pair (fidelity near 1) or a multi-bypassing long pair (fidelity near 0.5) yields a low efficiency. Thus, selecting an appropriate length to generate entangled pairs with moderate fidelity is crucial. 2) *Limited resources*. Even if the optimal length for purification is identified, nodes may not have sufficient resources to prepare an adequate number of sacrifice pairs. This limitation could hinder the purification process and compromise the achievement of desired fidelity levels. 3) *Trade-off between fidelity and probability*. The entangled pair's fidelity directly impacts the outcome of teleportation, so setting a fidelity threshold becomes essential. Higher fidelity necessitates more purification processes, which can cause lower probabilities conversely, as the scenario in Fig. 1(c) exemplifies. Thus, excessive purification processes may not be necessary when the fidelity threshold is already satisfied.

To address the above challenges, we introduce a novel optimization problem termed **D**ecoherence-aware **O**ptical Switch Assisted **S**wapping and **P**urify Optimization (DOSP). We discuss the related work in Section II and provide an overview of our system model and the formal definition of the DOSP in Section III. To tackle the DOSP, we propose a $(1-\delta)$-approximation algorithm named **N**ear-Optimal **S**wapping and **P**urifying **S**trategy Algorithm (NSPS) to jointly consider the probability and fidelity, identifying the near-optimal solution under a given fidelity threshold in Section IV. Then, the simulation results manifest that the NSPS outperforms the other methods, such as Q-LEAP [4] and Q-PATH [4], in Section V. Finally, we conclude this paper in Section VI.

II. Related Work

Recently, QN routing optimization has become a promising research topic. Shi *et al.* devised the Q-CAST routing method, using the Dijkstra algorithm to establish primary and recovery paths, mitigating entanglement failures [5]. Huang *et al.* considered trusted nodes and adopted social networks among users into the model [6]–[8]. Zhao *et al.* introduced the REPS algorithm, employing linear programming (LP) to optimize throughput in quantum networks [9]. Chen *et al.* proposed heuristics for entangling and swapping phases separately [10]. Chakraborty *et al.* gave an LP model to maximize the entanglement distribution rate [11]. However, no one considers fidelity decoherence with distance.

Zhao *et al.* suggested establishing longer entangled pairs via all-optical switching without conducting swapping at intermediate nodes [12]. However, they does not address fidelity loss with distance or purification processes. By contrast, Zhao *et al.* explored entangled links' fidelity, leveraging quantum purification to enhance link fidelity [13]. Li *et al.* utilized purification to meet fidelity requirements for multiple entangled pairs [4]. Nevertheless, the above work does not consider all-optical-switching and distance-related decoherence.

III. System Model and Problem Formulation

A. System Model

A quantum network with a central controller can be modeled by a graph $G = (V, E)$, where V is the set of $|V|$ quantum nodes and E is the set of $|E|$ quantum channels. The central controller facilitates classical communication and possesses complete information about all nodes, enabling it to coordinate their actions effectively. Each node $u \in V$ has limited quantum memory with a size of $c(u) \in \mathbb{Z}^+$, and each edge $(u, v) \in E$, connecting two adjacent nodes u and v, has sufficient quantum channel capacity (e.g., a bundle of optical fibers) to generate any desired number of entangled pairs between u and v.

Each node is equipped with the all-optical-switching technology to bypass quantum signals to non-adjacent nodes [12]. However, the signal-noise ratio (SNR) diminishes as a qubit traverses through a quantum channel. Thus, the success probability of generating an entangled link (i.e., entangling) decreases exponentially with the length of the channel, as described by the equation:

$$P_e(l(u,v)) = e^{-\alpha \cdot l(u,v)}, \tag{1}$$

where $l(u, v)$ is the optical path length between u and v, and α is a given constant based on the optical fiber's material [2]. During the entangling process, errors can occur, such as bit-flip errors, causing decoherence and fidelity loss. The fidelity of the binary entangled pair can be described by the equation:

$$F_e(l(u,v)) = \frac{1}{2} + \frac{1}{2} \cdot e^{-\beta \cdot l(u,v)}, \tag{2}$$

where $F_e(l(u, v))$ denotes the fidelity of the entangled pair between u and v, and β is a given constant based on various factors, e.g., position-dependent dephasing, imperfect atomic state preparation and readout, and detector dark-counts [14].

[1] In this example, we set the parameter α and the swapping probability for all nodes to 0.0002 and 0.85. The formula will be detailed in Section III-A.

To mitigate fidelity loss, entanglement purification is introduced to merge two low-fidelity pairs into a single higher-fidelity pair [3], [15]. It can be envisaged that one pair is the sacrifice pair, while the other is the target pair. This process can be realized using CNOT gates or optically using polarizing beamsplitters. The success probability of purification is [15]:

$$P_p(F_1, F_2) = F_1 \times F_2 + (1 - F_1) \times (1 - F_2), \tag{3}$$

where F_1 and F_2 are the fidelity of the two binary entangled pairs. Upon successful purification, the sacrifice pair is consumed, and the target pair achieves a new fidelity [15] by:

$$F_p(F_1, F_2) = \frac{F_1 \times F_2}{F_1 \times F_2 + (1 - F_1) \times (1 - F_2)}. \tag{4}$$

By contrast, both pairs are consumed in the event of failure, underscoring the inherent risks and uncertainties involved in the entanglement purification process.

Furthermore, one pair can be retained over several rounds and repeatedly purified with a base pair to achieve a higher fidelity. That purification technique is called pumping [15]. The fidelity and probability of employing the pumping method for n entangled pairs between nodes u and v are shown as follows:

$$\mathrm{F}(u, v, n) = \begin{cases} F_p(\mathrm{F}(u, v, n-1), F_e(l(u, v)) & \text{if } n > 1 \\ F_e(l(u, v)) & \text{if } n = 1 \end{cases} \tag{5}$$

$$\mathrm{P}(u, v, n) = \begin{cases} P_p(\mathrm{F}(u, v, n-1), F_e(l(u, v)) \\ \quad \cdot P_e(l(u, v)) \cdot \mathrm{P}(u, v, n-1) & \text{if } n > 1 \\ P_e(l(u, v)) & \text{if } n = 1 \end{cases} \tag{6}$$

Eqs. (5) and (6) are the recursion of fidelity and probability for the pumping method [15], respectively, where the fidelity and probability of entangled pairs are updated based on the results of previous purification rounds.

Entanglement swapping is a pivotal technique to merge two short entangled pair into a longer entangled pair. Conducting swapping on node u has a success probability $Q(u)$ to merge an entangled pair (x, u) with fidelity F_1 and another one (u, y) with fidelity F_2 into a longer pair (x, y) with fidelity $F_1 \times F_2$ [15]. This process facilitates merging entangled pairs for distant nodes, extending the entanglement over larger distances within the quantum network.

B. Time-Slotted Quantum Network System

In this paper, we consider a time-slotted QN system. Each time slot can be broadly divided into four phases as follows:

1) Request dealing phase: At the beginning of each time slot, a request r with its specified path $(s, v_1, v_2, ..., d)$ arrives. The controller assesses the resources along the path to devise a strategy for generating entangled pairs to derive an end-to-end pair that meets the fidelity threshold specified by the request.

2) Entangling phase: The entangled pairs are generated according to the devised strategy. Note that some of them may opt to bypass certain nodes, as shown in Figs. 1(b) and 1(c). The entanglement success probability can be determined by Eq. (1). Upon success, each pair has fidelity as described by Eq. (2) and occupies one quantum memory on each node involved.

3) Purifying phase: Node u and node v undergo purification with the entanglement pumping method to merge the entangled pairs generated between u and v for request r into a single pair.

4) Swapping phase: The nodes on the path execute swapping processes to merge the purified pairs into an end-to-end pair for request r.

C. Problem Formulation – DOSP

Consider the routing path $V = (v_1, v_2, ..., v_{|V|})$ for request r, where each node $u \in V$ has memory limit $c(u) \in \mathbb{Z}^+$ and a swapping success probability $\mathrm{Q}(u) \in (0, 1]$. For ease of reading, we additionally let s and d denote v_1 (i.e., the source) and $v_{|V|}$ (i.e., the destination), respectively. The DOSP asks for a bypassing and purifying strategy to connect s and d and maximize the success probability with following constraints.

1) The fidelity of the generated end-to-end pair by the strategy must satisfy the fidelity threshold F_T.
2) The amount of used memory at each node $u \in V$ does not exceed its memory size $c(u)$.

Let $\rho(u)$ denote the visiting order of node u on the path. That is, node u is the $\rho(u)$-th visited node on the path. Thus, if $\rho(u) < \rho(v)$, then the path visits u earlier than v. For ease of presentation, let $m(u, v) = \min\{c(u), c(v)\}$. The DOSP can be formulated as an integer programming (IP) (7a)-(7g), with the binary decision variable $x^n_{u,v} \in \{0, 1\}$ denoting whether to build n entangled pairs between u and v:

$$\max \prod_{\substack{u,v \in V: \\ \rho(u) < \rho(v)}} \prod_{n=1}^{m(u,v)} \mathrm{P}(u, v, n)^{x^n_{u,v}} \prod_{\substack{u,v \in V: \\ \rho(u) < \rho(v), \\ u \neq s}} \prod_{n=1}^{m(u,v)} \mathrm{Q}(u)^{x^n_{u,v}} \tag{7a}$$

$$\text{s.t.} \prod_{u,v \in V: \rho(u) < \rho(v)} \prod_{n=1}^{m(u,v)} \mathrm{F}(u, v, n)^{x^n_{u,v}} \geq F_T \tag{7b}$$

$$\sum_{\substack{u,v \in V: \rho(u) < \rho(v), \\ u = j || v = j}} \sum_{n=1}^{m(u,v)} n \cdot x^n_{u,v} \leq c(j), \ \forall j \in V \tag{7c}$$

$$\sum_{v \in V \setminus \{s\}} \sum_{n=1}^{m(s,v)} x^n_{s,v} - \sum_{v \in V \setminus \{s\}} \sum_{n=1}^{m(v,s)} x^n_{v,s} = 1 \tag{7d}$$

$$\sum_{v \in V \setminus \{u\}} \sum_{n=1}^{m(u,v)} x^n_{u,v} = \sum_{v \in V \setminus \{u\}} \sum_{n=1}^{m(v,u)} x^n_{v,u}, \ \forall u \in V \tag{7e}$$

$$\sum_{v \in V \setminus \{d\}} \sum_{n=1}^{m(d,v)} x^n_{d,v} - \sum_{v \in V \setminus \{d\}} \sum_{n=1}^{m(v,d)} x^n_{v,d} = -1 \tag{7f}$$

$$x^n_{u,v} \in \{0, 1\}, \qquad \forall u, v \in V, \rho(u) < \rho(v) \tag{7g}$$

The objective function (7a) aims to find the strategy that maximizes the success probability of the routing path for request r. Constraint (7b) guarantees that the fidelity satisfies the threshold F_T. Constraint (7c) ensures that the amount of

used memory at each node j does not exceed the memory limit $c(u)$ on node u. Constraints (7d)-(7f) guarantee the generated entangled pair is end-to-end from s to d if it succeeds.

IV. Algorithm Design – NSPS

In the literature, there are two related algorithms, the Q-LEAP [4] and Q-PATH [4], which can be applied to acquire feasible solutions of the DOSP. The Q-LEAP generate a sufficient number of sacrifice pairs for purification to acquire an entangled pair with fidelity of at least $\sqrt[h]{F_T}$ between any two neighboring nodes on the path, where h is the number of edges on the path. In this way, the end-to-end pair with sufficient fidelity (i.e., satisfying the threshold) can be acquired after the repeaters conducting swapping. However, increasing the fidelity individually makes the Q-LEAP easily fall into the local minimum. By contrast, the Q-PATH iteratively examines every edge on the path and adds the entangled pair (as an sacrifice pair) that can increase the overall fidelity most for purification until the fidelity threshold is satisfied. This design helps the Q-PATH outperform the Q-LEAP. Nonetheless, both they neglect the impact on the fidelity of the quantum channel length due to decoherence and the promising bypassing technology.

To efficiently solve the DOSP, we propose a novel algorithm named **N**ear-Optimal **S**wapping and **P**urifying **S**trategy Algorithm (NSPS) to overcome the challenges and achieve the optimum solution. The idea is to construct a weighted directed *auxiliary graph* $\hat{G} = \{\hat{V}, \hat{E}\}$, where each virtual path from the virtual source $\hat{s}$ to the virtual destination $\hat{d}$ corresponds a bypassing and purifying strategy for generating the end-to-end entangled pair for request r. To this end, multiple duplicate virtual nodes are created and added to the auxiliary graph $\hat{G}$ for each node $u \in V$. Each duplicate virtual node $\hat{v}_u^i$ indicates the amount of memory of node u would be consumed (i.e., $i = 0, 1, ..., c(u)$) for entangling and purification before the strategy between u and its next-hop node is determined. Meanwhile, each weighted virtual edge $(\hat{v}_u^i, \hat{v}_v^j)$ created and added to $\hat{E}$ represents a strategy applied to u and v in V. Selecting virtual edge $(\hat{v}_u^i, \hat{v}_v^j)$ implies that j entangled pairs (i.e., one target pair and $j-1$ sacrifice pairs) are generated between u and v for deriving an entangled pair with the fidelity $\mathrm{F}(u, v, j)$ and probability $\mathrm{P}(u, v, j)$. Subsequently, the NSPS introduces the *fidelity cost* and *probability cost* for each virtual edge, which are additive and mapped from the fidelity and the probability of the generated entangled pair guided by $(\hat{v}_u^i, \hat{v}_v^j)$. The lower the fidelity cost (or the probability cost), the higher the fidelity (or the probability). Last, the NSPS adopts a polynomial-time approximation scheme (PTAS) for the restricted shortest path (RSP) [16] to find a path from $\hat{s}$ to $\hat{d}$ with the near-minimum probability cost while ensuring the induced fidelity cost is no greater than a threshold, deriving the near-optimum strategy.

The NSPS includes two phases: 1) Auxiliary Graph Construction (AG Construction) and 2) Near-optimal Strategy Establishment (NS Establishment). In the AG Construction, NSPS constructs an auxiliary graph $\hat{G}$ such that every virtual path from the virtual source to the virtual destination has a corresponding bypassing and purifying strategy. In the NS Establishment, NSPS converts the fidelity and probability to fidelity cost and probability cost for edges in $\hat{G}$ and solve the converted problem with the PTAS of the RSP [16]. Finally, NSPS returns the bypassing and purifying strategy corresponding to the found path in $\hat{G}$.

A. Auxiliary Graph Construction (AG Construction)

For every node $u \in V$, as shown in Fig. 2(a), the NSPS first generates multiple duplicate virtual nodes and add them to $\hat{V}$, as shown in green nodes of Fig. 2(b). Note that each duplicate virtual nodes $\hat{v}_u^i$ represents the memory with a size of i is consumed for entangling and purification before the strategy between u and its next-hop node is determined. Thus, the source $\hat{v}_1$ (i.e., s) has only one virtual node, $\hat{v}_1^0$. By contrast, each node $u \in V \setminus \{v_1\}$ has virtual nodes $\hat{v}_u^1, ..., \hat{v}_u^{c(v)}$ but $\hat{v}_u^0$. Subsequently, for each pair of nodes u and v in V, where $\rho(u) < \rho(v)$, the NSPS creates a virtual edge between $\hat{v}_u^i$ and $\hat{v}_v^j$ and then adds it to $\hat{E}$ if $c(u) \geq i + j$ and $c(v) \geq j$, as shown in red lines of Figs. 2(c) and 2(d).

To set the fidelity $\hat{\mathrm{F}}(\hat{v}_u^i, \hat{v}_v^j)$ and probability $\hat{\mathrm{P}}(\hat{v}_u^i, \hat{v}_v^j)$ for each virtual edge $(\hat{v}_u^i, \hat{v}_v^j) \in \hat{E}$, where $\rho(u) < \rho(v)$, the NSPS exploits the following equations.

$$\hat{\mathrm{F}}(\hat{v}_u^i, \hat{v}_v^j) = \mathrm{F}(u, v, j) \tag{8}$$

$$\hat{\mathrm{P}}(\hat{v}_u^i, \hat{v}_v^j) = \begin{cases} \mathrm{P}(u, v, j), & \text{if } v = d \\ \mathrm{P}(u, v, j) \cdot \mathrm{Q}(v), & \text{if } v \neq d \end{cases} \tag{9}$$

Note that in Eq. (9), if v is the destination of request r, then no swapping is needed at v; otherwise, the swapping to connect the two entangled pairs of v is required. Finally, the NSPS sets $\hat{v}_1^0$ as the virtual source $\hat{s}$, adds a virtual destination $\hat{d}$ to $\hat{V}$, and adds the virtual edge between each virtual node of $v_{|V|}$ to $\hat{d}$, as shown in Fig. 2(e).

B. Near-optimal Strategy Establishment (NS Establishment)

After the AG Construction, the optimization problem (7a)-(7g) can be solved by finding the virtual path p from $\hat{s}$ to $\hat{d}$ in $\hat{G}$ such that the fidelity is no less than the threshold F_T while the probability is maximized. Let $\mathcal{P}(\hat{s}, \hat{d})$ denote the set of all possible paths between $\hat{s}$ and $\hat{d}$ in $\hat{G}$. Thus, it is equivalent to compute:

$$\max_{p \in \mathcal{P}(\hat{s}, \hat{d})} \prod_{(\hat{v}_u^i, \hat{v}_v^j) \in p} \hat{\mathrm{P}}(\hat{v}_u^i, \hat{v}_v^j) \tag{10a}$$

$$\text{s.t.} \prod_{(\hat{v}_u^i, \hat{v}_v^j) \in p} \hat{\mathrm{F}}(\hat{v}_u^i, \hat{v}_v^j) \geq F_T \tag{10b}$$

However, the number of paths in $\mathcal{P}(\hat{s}, \hat{d})$ could grow exponentially with the number of virtual nodes. To overcome the difficulty, by the PTAS of the RSP [16], we can acquire the near-optimal solution, i.e., our solution $P_{ALG} \geq (1-\delta)P_{OPT}$, where $\delta > 0$, if satisfying the property: the probability cost and fidelity cost are non-negative and additive.

To meet the property, the NSPS sets the probability cost and fidelity cost for each edge $(\hat{v}_u^i, \hat{v}_v^j) \in \hat{E}$ as follows.

$$\mathbb{F}(\hat{v}_u^i, \hat{v}_v^j) = -\ln \hat{\mathrm{F}}(\hat{v}_u^i, \hat{v}_v^j) \text{ and } \mathbb{P}(\hat{v}_u^i, \hat{v}_v^j) = -\ln \hat{\mathrm{P}}(\hat{v}_u^i, \hat{v}_v^j)$$

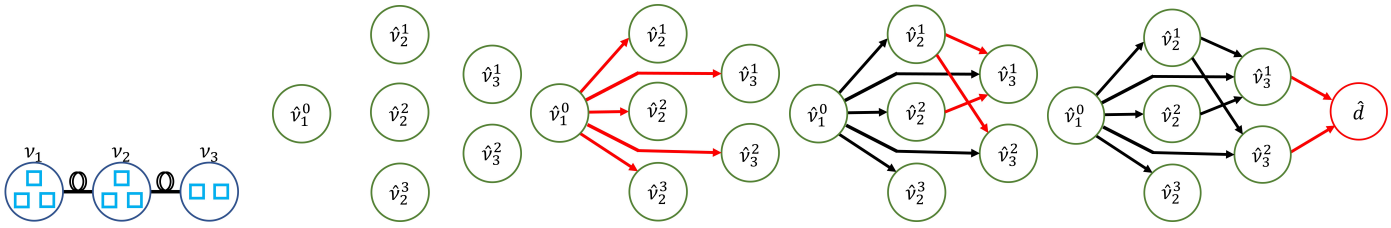

(a) Given routing path (b) Duplicate virtual nodes (c) Create $\hat{v}_1^0$'s virtual edges (d) Create $\hat{v}_2^1$'s virtual edges (e) Auxiliary graph

Fig. 2. An example of the construction of an auxiliary graph for the given routing path.

After setting the two costs, the optimization problem (10a)-(10b) can be rewritten as the following form for the RSP.

$$\min_{p\in\mathcal{P}(\hat{s},\hat{d})} x(p) \coloneqq \sum_{(\hat{v}_u^i,\hat{v}_v^j)\in p} \mathbb{P}(\hat{v}_u^i,\hat{v}_v^j). \tag{11a}$$

$$\text{s.t. } y(p) \coloneqq \sum_{(\hat{v}_u^i,\hat{v}_v^j)\in p} \mathbb{F}(\hat{v}_u^i,\hat{v}_v^j) \le -\ln F_T. \tag{11b}$$

We can employ the PTAS of the RSP [16] to find a solution p_{ALG} with $x(p_{ALG}) \le (1+\epsilon)\cdot x(p_{OPT})$, where p_{OPT} is the optimal path for the DOSP and ϵ is a positive user-defined constant. Subsequently, we show that a near-optimum for the DOSP can be derived by properly setting ϵ as follows.

Theorem 1. To acquire a $(1-\delta)$-approximation algorithm for the DOSP, where δ is a positive user-defined constant, we can set the positive user-defined constant ϵ for the PTAS of the RSP [16] by the following equation, where p_f is the path with the lowest fidelity cost, i.e., $y(p_f) \le y(p)$, $p \in \hat{G}$.

$$\epsilon = \frac{-\ln(1-\delta)}{x(p_f)} \tag{12}$$

Proof. Let P_{ALG} and P_{OPT} denote the probability of the path p_{ALG} and the probability of the optimal path p_{OPT} for the DOSP, respectively. By using the PTAS of the RSP [16], we have $x(p_{ALG}) \le (1+\epsilon)\cdot x(p_{OPT})$. Therefore, we know that:

$$\begin{aligned} P_{ALG} &= e^{-x(p_{ALG})} \ge e^{-(1+\epsilon)\cdot x(p_{OPT})} \\ &= P_{OPT}\cdot e^{-x(p_{OPT})\cdot\frac{-\ln(1-\delta)}{x(p_f)}} \\ &\ge P_{OPT}\cdot e^{\frac{x(p_{OPT})}{x(p_{OPT})}\cdot\ln(1-\delta)} = (1-\delta)\cdot P_{OPT} \end{aligned}$$

Note that the last inequality is true since $x(p_{OPT}) \le x(p_f)$ and $\ln(1-\delta)$ is a negative value. □

Note that the path with the lowest fidelity cost (i.e., p_f) can be found by the Dijkstra algorithm in polynomial time. Thus, ϵ can be acquired in polynomial time.

V. Performance Evaluation

A. Simulation Settings

We follow the setting for the Waxman model in [4] to generate the networks for comparing our algorithm (i.e., the NSPS with the user-defined constant $\delta = 0.7$) with the Q-PATH and the Q-LEAP [4]. We adjust only one parameter as the independent variable for each simulation; the default setting is as follows. For each network, we randomly deploy five nodes within a 250 km × 250 km area. The amount of node memory is randomly set between 5 and 9. The success probability of swapping at each node is set to 0.7, and the fidelity threshold is set to 0.85. The channel length $l(u,v)$ between two adjacent nodes u and v are calculated by Euclidean distance. We set $\alpha = 0.0002$ and $\beta = 0.0044$ in $P_e(l(u,v))$ and $F_e(l(u,v))$. Each result is averaged over 50 trials.

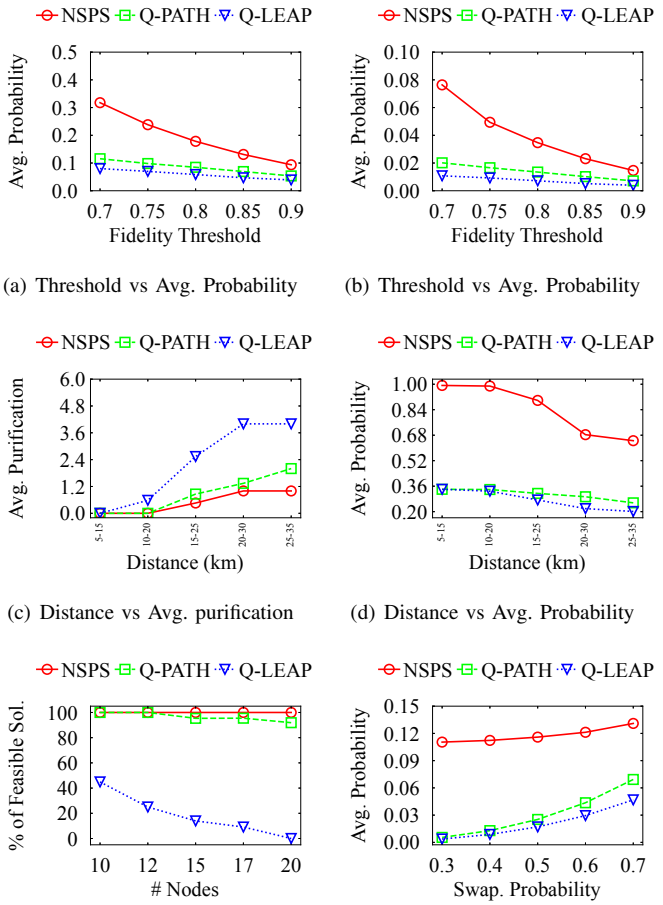

(a) Threshold vs Avg. Probability (b) Threshold vs Avg. Probability

(c) Distance vs Avg. purification (d) Distance vs Avg. Probability

(e) # Nodes vs % of Feasible sol. (f) Swap Prob. vs Avg. Probability

Fig. 3. Effect of different parameters on different metrics.

B. Numerical Results

1) Effect of Fidelity on Success Probability: Figs. 3(a) and 3(b) illustrate the average success probability of requests with 5 and 7 nodes at different fidelity thresholds, respectively. The success probability decreases as the fidelity threshold increases because a higher fidelity threshold requires more purification

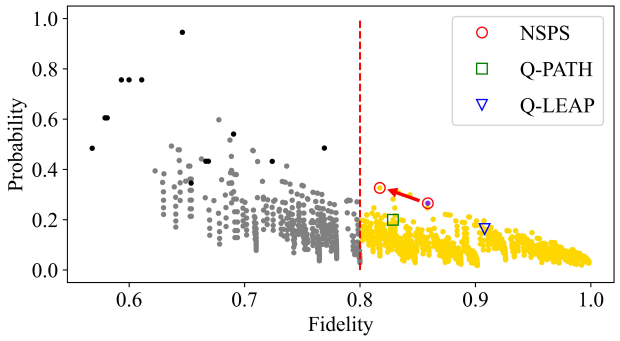

Fig. 4. Effect of memory size on success probability. Purple / black points present the original feasible / infeasible solutions. Yellow / grey points indicate additional feasible / infeasible solutions when the memory size increases.

processes to meet the constraint. The NSPS outperforms the Q-PATH and Q-LEAP by at least 77% and 141%, respectively. This indicates that the NSPS can strike a balance between fidelity and probability and address the third challenge.

2) Effect of Adjacent Node Distance: Fig. 3(c) shows the effect of nodes distance on average number of purification processes. The request with a longer distance between nodes has low fidelity of entangled pairs and requires more purification processes to meet the fidelity threshold. The NSPS needs fewer purification processes than the Q-PATH and Q-LEAP to meet the fidelity threshold so that it suffers from a lower probability loss. This indicates that the NSPS can effectively address the first challenge. On the other hand, Fig. 3(d) compares the success probability at different distances. Since the NSPS performs fewer number of purification, its success probability is higher than those of the Q-PATH and Q-LEAP.

3) Effect of the Number of Nodes on Generation Rate of Feasible Solutions: Fig. 3(e) illustrates the impact of number of nodes on the generation rate of feasible solutions for different algorithms. The Q-LEAP delivers a generation rate of 50% even if the number of nodes is 10 and exhibits a substantial decrease as the number of nodes increases. On the other hand, the Q-PATH maintains a generation rate of 100% as there are 12 nodes, but the rate drops when there are 15 nodes. By contrast, the NSPS consistently achieves a generation rate of 100%. This consistency highlights the robustness and scalability of the NSPS, making it superior in handling larger network scales. This analysis underscores the critical role of algorithm design in managing increased network complexities and maintaining higher performance standards.

4) Effect of Swapping Probability: Fig. 3(f) explores the relation between swapping probability and overall success probability for different algorithms. Overall, a lower given swapping probability results in a lower overall success probability. However, the results also show that both the Q-PATH and Q-LEAP exhibit a directer correlation between the swapping probability and overall probability. This is because they lack the consideration bypassing techniques. In contrast, the NSPS demonstrates less dependency on the swapping probability. Even with lower swapping probability (e.g., 0.3 and 0.4), the NSPS maintains a relatively high overall success probability. This numerical analysis highlights the robustness of NSPS in maintaining performance consistency across varying levels of swapping probabilities, underscoring its effectiveness in scenarios where swapping might be less reliable.

5) Effect of Memory size: Fig. 4 describes the effect of memory size on the solution quality, where $F_T = 0.8$. When the memory is scarce, the NSPS can find the optimum (purple point), while the Q-PATH and Q-LEAP cannot find any solution. As the memory increases, more feasible solutions with higher probabilities (yellow points) emerge. Thus, the NSPS can find a better feasible solution with the highest overall success probability. However, the Q-PATH and Q-LEAP can only find the feasible solutions with a lower success probability. This demonstrates that the NSPS can handle the second challenge better than the Q-PATH and Q-LEAP.

VI. Conclusion

This paper introduces a novel optimization problem called DOSP to maximize the success probability of constructing end-to-end entangled pairs while satisfying fidelity constraints. The DOSP aims to identify a swapping and purification strategy to make good use of all-optical-switching bypassing and purification processes under the memory capacity constraints. To address the DOSP, we propose a new $(1-\delta)$-approximation algorithm NSPS to jointly consider the success probability and induced fidelity. Finally, simulation results demonstrate that the NSPS outperforms existing methods by at least 70%.

References

[1] M. A. Nielsen and I. Chuang, *Quantum computation and quantum information*. American Association of Physics Teachers, 2002.
[2] N. Sangouard, C. Simon, H. De Riedmatten, and N. Gisin, "Quantum repeaters based on atomic ensembles and linear optics," *Rev. Mod. Phys.*, vol. 83, no. 1, p. 33, 2011.
[3] J.-W. Pan *et al.*, "Entanglement purification for quantum communication," *Nature*, vol. 410, pp. 1067–1070, 2001.
[4] J. Li *et al.*, "Fidelity-guaranteed entanglement routing in quantum networks," *IEEE Trans. Commun.*, 2022.
[5] S. Shi and C. Qian, "Concurrent entanglement routing for quantum networks: Model and designs," in *ACM SIGCOMM*, 2020.
[6] S.-M. Huang *et al.*, "Socially-aware concurrent entanglement routing with path decomposition in quantum networks," in *IEEE GLOBECOM*, 2022.
[7] ——, "Socially-aware concurrent entanglement routing in satellite-assisted multi-domain quantum networks," in *IEEE ICC*, 2023.
[8] ——, "Socially-aware opportunistic routing with path segment selection in quantum networks," in *IEEE GLOBECOM*, 2023.
[9] Y. Zhao and C. Qiao, "Redundant entanglement provisioning and selection for throughput maximization in quantum networks," in *IEEE INFOCOM*, 2021.
[10] L. Chen *et al.*, "A heuristic remote entanglement distribution algorithm on memory-limited quantum paths," *IEEE Trans. Commun.*, vol. 70, no. 11, pp. 7491–7504, 2022.
[11] K. Chakraborty, D. Elkouss, B. Rijsman, and S. Wehner, "Entanglement distribution in a quantum network: A multicommodity flow-based approach," *IEEE Trans. Quantum Eng.*, vol. 1, pp. 1–21, 2020.
[12] G. Zhao, J. Wang, Y. Zhao, H. Xu, L. Huang, and C. Qiao, "Segmented entanglement establishment with all-optical switching in quantum networks," *IEEE ACM Trans. Netw.*, vol. 32, no. 1, pp. 268–282, 2024.
[13] Y. Zhao *et al.*, "E2E fidelity aware routing and purification for throughput maximization in quantum networks," in *IEEE INFOCOM*, 2022.
[14] T. van Leent *et al.*, "Long-distance distribution of atom-photon entanglement at telecom wavelength," *Phys. Rev. Lett.*, vol. 124, no. 1, p. 010510, 2020.
[15] R. Van Meter, *Quantum Networking*. John Wiley & Sons, Ltd, 2014.
[16] F. Ergun, R. Sinha, and L. Zhang, "An improved FPTAS for restricted shortest path," *Inf. Process. Lett.*, vol. 83, no. 5, pp. 287–291, 2002.